

Article | Received 14 November 2024; Accepted 17 February 2025; Published date
<https://doi.org/10.55092/XXXX>

A study on a tactile display drive system using SPI communication and a piezoelectric driver IC

Junyun Zheng¹, Yuya Otahara¹ and Junji Sone^{2,*}

¹ Graduate School of Engineering, Tokyo Polytechnic University, Atsugi, Kanagawa, Japan

² Faculty of Engineering, Tokyo Polytechnic University, Atsugi, Kanagawa, Japan

* Correspondence author: Junji Sone; E-mail: sone@eng.t-kougei.ac.jp.

Highlights:

- Sensation through haptic devices
- Miniaturization of driver circuits for wearable devices
- Device output control by digital dither

Abstract: Tactile technology is becoming increasingly important due to robotics applications and the use of the metaverse. However, there is few research on tactile technologies that can provide information on two-point discrimination thresholds at the human sensory level, and practical application has not progressed. This is due to the fact that the devices are complex and cannot be compactly mounted in key locations such as fingertips. This research aims to develop thin, flexible piezoelectric resin devices and put them into practical use. Here, it is important to miniaturize the drive circuits that drive such piezoelectric devices, so we developed a drive system that uses a piezoelectric driver IC that utilizes serial communication, and is capable of generating a wide range of tactile sensations, including multi-tone gradations.

Keywords: tactile display; drive system; SPI communication; piezoelectric driver IC; two-point discrimination; flexible piezoelectric resin device

1. Introduction

Virtual Reality [1,2] first appeared in 1960 with the Telesphere Mask, which was the first head-mounted display. In the 1980s, VPL Research released an HMD called the Eyephone, and then a glove-shaped input device called The Data Glove appeared. In the 2010s, Oculus Rift, HTC Vive, and Sony's Playstation VR appeared. Meanwhile, Microsoft announced the HoloLens, a device for mixed reality (MR) [3], which makes it possible to overlay various images onto reality. In Japan, Tachi [4–9] and Hirose [10,11] have been conducting research into VR since the 1980s, advancing research into the fields



Copyright©2025 by the authors. Published by ELSP. This work is licensed under Creative Commons Attribution 4.0 International License, which permits unrestricted use, distribution, and reproduction in any medium provided the original work is properly cited.

of vision, touch, and teleoperation. And this research is becoming increasingly important across a wide range of fields, including applications in VR, AR, medicine, and robotics.

In recent years, haptic [12] and tactile [13] technology has rapidly developed. Human touch is composed of mechanical, sensory, motor and cognitive elements, where sensory mechanisms are activated by physical stimuli and messages are perceived by the brain. Sense of touch is made up of Haptic and Tactile. Haptic is realized by providing deep sensations in the joints of the hands and arms and pressure sensations to the fingers. Tactile is realized by giving shape, roughness and texture to the fingertips. This is done by generating algorithms to place objects in the virtual environment and touch them with virtual fingers. The two key elements are visual rendering, which presents information about the virtual environment to the user, and haptic rendering. Haptic rendering is responsible for presenting the contact location to the human, both visually and by force. Phantom [14] is a well-known haptic device developed for industrial, medical, and scientific applications. However, it can only present a single point of force sensation to the entire hand. In Japan, Iwata and Sato are pioneers, with Iwata developing Haptic Master [15] and Sato developing SPIDAR [16–17], both of which are world famous. To solve the problem of single-point presentation, the multi-fingered haptic displays were created, Sato's SPIDAR [18–19] and Kawasaki's side-faced-type multi-fingered haptic interface [20]. And we also developed a multi-fingered haptic device that can present an encounter-type haptic sensation to three fingers [21]. In reality, to achieve an accurate virtual reality experience, it is necessary to accurately present both the sense of haptic and the sense of tactile, but in this research, the emphasis is on the sense of tactile. In the next step, we will consider presenting tactile and haptic simultaneously.

Tactile displays have the function of presenting the shape, surface roughness, and texture of objects to humans. Humans have layers under the skin: epidermis, dermis, and subcutaneous tissue [22]. The epidermis is 0.4 to 2.0 mm thick, and the second layer, the dermis, is 5–10 mm thick and is located under the epidermis. The dermis contains blood vessels, lymphatic vessels, nerve fibers, and many sensory nerve endings. To sense touch, the skin has seven types of mechanoreceptors and four types of pain receptors. When analyzing each type, it is necessary to provide information that matches these to construct a tactile display. Each of these receptors is located at a specific depth in the skin. In fingers and hands, the shallowest Meissner's corpuscles are 0.7 mm below the surface and sense stroking and fluttering. The frequency is 10–300 Hz, but the sensitivity is high at 200–300 Hz. The Merkel disk receptor senses pressure and texture, senses frequencies of 0.4–100 Hz, and is located 0.5–1.0 mm deep. The Pacinian corpuscle senses vibrations at 40–800 Hz, but is more sensitive at 200–300 Hz and is located about 2 mm deep from the surface. The Ruffini ending senses skin expansion and contraction of the skin at a frequency of 7 Hz and is located about 2 mm deep from the surface. The characteristics of each receptor show that in order to stimulate these mechanoreceptors and obtain a sense of touch, it is effective to first provide a 200 Hz–300 Hz instructional stimulus.

In particular, multi-point tactile and haptic devices that can simultaneously control multiple contact points are expected to be used in applications that require precise tactile feedback. Tactile technology is also being applied to remote control and the medical field, expanding its potential as a new interface. In addition, tactile and haptic presentation devices incorporate the sense of touch in addition to sight and hearing, providing a more immersive experience.

Several dynamic and static devices have been developed for the research of tactile device [23]. The optical character reader Optacon was developed to present Braille to the visually impaired. It has a 6×24

array of actuators with a pitch of 1.1 to 2.1 mm and operates at up to 250 Hz, but is fixed in place [24]. The actuators are quite large, and the pins are integrated to ensure resolution. Ikei *et al.* developed pin array with 11×6 pins arranged with a pitch of 2 mm for a vibration, driven by stacked piezoelectric actuators and mechanically amplified by a cantilever beam. It can present stimuli at 230–700 Hz, achieving high speed and density [25]. Hudin has also developed a thin glass plate device that generates tactile friction on the surface [26]. However, these systems have big moving parts and are not suitable for wearable.

High density and lightweight device suitable for wearable applications, Kajimoto group developed an electrotactile display using pulse width modulation with real-time impedance feedback [27]. This technology directly stimulates sensory nerves via electrodes placed on the surface of the skin. However, there are issues with the stability of the presented sensation, and factors that cause this include temporary fluctuations due to sweat or changes in skin contact conditions, and spatial variation in the stimulation threshold between electrodes. In particular, when using multiple electrodes, the small difference between the absolute threshold and the pain threshold becomes an issue, and real-time impedance feedback technology has been proposed to reduce the variation in sensation. This technology improves the spatial and temporal stability of the presented sensation by measuring the skin resistance and dynamically adjusting the stimulation pulse width based on that data. Here, vibration frequencies between 10 Hz and 320 Hz are utilized. The relationship between each mechanoreceptor and electrical stimulation has been researched, but only pressure sensation has been confirmed, and the relationship with other sensations is still under research. Higashi *et al.*'s research has shown that the specific frequency range for hardness perception is that vibration frequencies around 200 Hz to 400 Hz have the greatest effect on human hardness perception [28].

As a soft actuator, Koo *et al.* developed flexible display using an electroactive polymer with a 5×4 array over an $11 \text{ mm} \times 14 \text{ mm}$ area, an actuator diameter of 2 mm, and a thickness of 3 mm [29]. The displacement was $100 \mu\text{m}$ and the operating frequency was 100 Hz. Although the device structure with soft and flexible characteristics was easy to fabricate, it required 2.5 kV voltage, and the displacement decreased significantly by increasing frequency. Lee *et al.* developed a dielectric elastomer flexible device using with a 2×3 array at 5 mm intervals [30]. Although the actuators had a large deformation, the tactile density was low and the response speed was slow at 10 Hz. Therefore, a tactile display that presents tactile sensations to multiple fingers needs to present a variety of information while meeting the requirements of compactness, density, and frequency. In this study, a high-speed thin-film resin device was used [31], in addition, the author is also developing an ultrasonic device [32].

Our group is also developing tactile devices, controlling such multi-point tactile sensations requires a lot of wiring. However, to achieve compactness, it is necessary to reduce the amount of wiring. To achieve this, it is advantageous to transmit control signals from the PC via serial communication [33]. And the piezoelectric amplifiers normally used PIEZO DRIVER / AMPLIFIER. Our group use a Trek MODEL PZD 350, but it is large and can only drive one channel. To achieve wearable, to install the driving circuit close to the device, we use high voltage output Integrated Circuit (IC). Here, Serial Peripheral Interface (SPI) is used for communication, and Microchip's 8-Channel Serial-to-Parallel Converter with High-Voltage Push-Pull Outputs: HV513 is used as the driving IC, which can control voltage up to 250V and drive piezoelectric devices. We also developed a control system on a PC that generates tactile patterns for each of the 25 tactile presentation points and changes the tactile patterns

over time. We also implemented a function to control the frequency at double the frequency so that dithering [34] can be performed, focusing on the strength of the tactile sensation.

2. Tactile Device

2.1. Overview of the tactile device

In the development of a multi-point tactile device, material selection and structural design are key steps. The tactile device developed in this study uses silicone rubber (Smooth-On, Inc. Ecoflex OO 30) and fluorinated ethylene propylene (FEP) film [35] as main structural materials, with Titanium (Ti) electrodes deposited on top for a flexible, durable structure by sputter (Shibaura mechatronics, CFS-4ES). Additionally, electrodes and wiring are formed by depositing Au or Cu, enhancing the device's durability and reliability using Electron beam evaporator (SANYU ELECTRON SVC-700 LEB/4G). Figure 1 shows a cross-sectional view of the tactile device. An FEP film is attached to the top, where a metal film electrode pattern is formed. The entire bottom side has a metal film electrode as earth electrode, and flexible silicone rubber is sandwiched in the center. The FEP film is 25 μm thick, the silicone rubber is 0.25 mm thick, and the total thickness is 0.3mm. The upper electrode connects to the positive terminal of the drive circuit, and the lower electrode connects to the earth ground terminal.

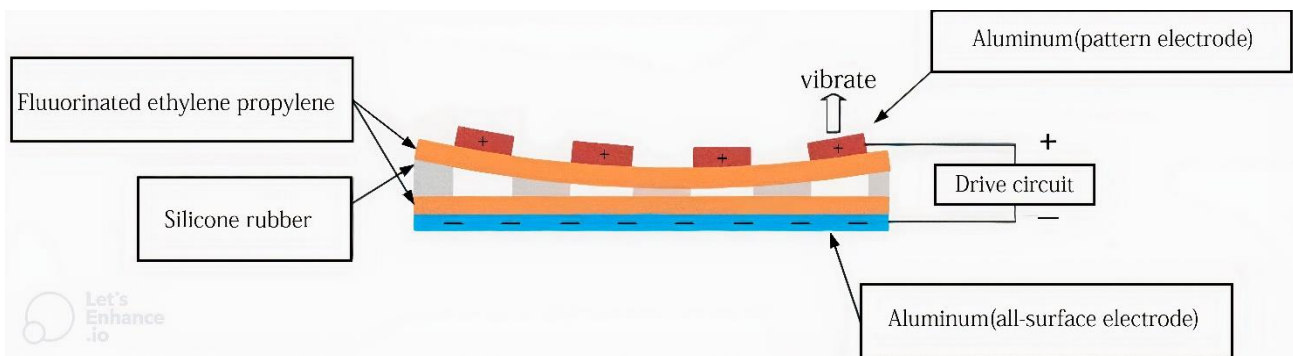


Figure 1. Cross-sectional structure of the Tactile device.

The device structure features 25 vibration generation points within a 2 cm \times 2 cm area. Each tactile generation point is independently controlled, allowing for different types of tactile patterns. Figure 2 shows the front and back surfaces of the tactile device. The circular area of the inner 2/3 of the area is the area that vibrates individually. The device is thin and flexible because it is made of polymer and silicone rubber.



(a) Front



(b) Back

Figure 2. Photograph of tactile device.

The device prototype was created by the following steps:

- (1) Using the spin coater flatten a silicon rubber film with a thickness of 0.2 mm. EcoFlex OO 30 was used to manufacture silicone rubber.
- (2) The FEP film and silicone rubber film were cleaned using oxygen plasma (100 W, 100 Pa, O₂: 30sccm) and 3-aminopropyl triethoxysilane (APTES) was used to bond the silicone rubber to the film. And the FEP film and the silicone rubber film were bonded 6 hours on a hot plate at 40 °C under the pressure of 200 g weight.
- (3) One side of the FEP film, a Ti electrode film of about 70 nm was deposited on one side of the multi-point device by sputtering. Other side of FEP film, a Ti electrode film of about 70 nm was deposited form a 2 cm square earth ground area.
- (4) One side of the FEP film on a 70 nm Ti electrode using sputtering, 200 to 300 nm Au or Cu wiring was deposited by EB evaporation. Other side of FEP film, 100 nm to 300 nm Au or Cu electrode film was deposited form a 2 cm square earth ground area.
- (5) A normal corona charge requires several tens of kV, we used 1KV for 20 minutes direct charging was performed at 120 °C by pressing between electrodes.

3. Control system configuration

3.1. Overall configuration of the control system

The control hardware of the tactile device primarily comprises a high-voltage push-pull output driver (HV513) with serial-to-parallel conversion and an Arduino. The Arduino transfers tactile generation data from a PC to the HV513 using SPI communication. HV513 converts serial data to parallel data and, with high-voltage push-pull output drivers that support up to eight output channels, it drives the piezoelectric control of the device, generating tactile sensations. Figure 3 shows the hardware circuit diagram. Using two DC-DC converters, MHV12-300S10P, a stable high voltage of 200V is supplied to the HV513 from 12 V source power.

This drive circuit is controlled by communicating control signals from a PC using an Arduino Mega 2560 to control the four HV513 (total 32 channel control). The control program employs a Bit-Banging control method that emulates SPI communication. Clock (CLK), data (DATA), and latch (LE) signals are sent from the Arduino GPIO pins to the HV513, enabling serial data transfer. The data is input bit by bit into the shift register synchronized with the clock's rising edge. After all data is transferred, the Arduino sets the latch signal (by sending a signal to the LE pin), transferring the data to the internal register of the HV513 and updating the high-voltage output signal. This setup enables simultaneous control of multiple tactile generation points. The Arduino ensures precise data transfer timing and generates the clock signal, controlling the frequency of vibration patterns. This mechanism allows various tactile feedback to be provided to the user.

Figure 4 shows the waveform of CLK, the DATA, and LE when transmitting the serial data "00100111" as an example. The CLK determines the timing of data transfer, and a bit pattern, such as "00100111," is sent as the DATA. After all data is transferred, the LE is set, transferring the data to the output register and sending it to each channel. By repeating this process, the output of 25 tactile

generation points can be updated and controlled with precise timing. This setup allows 25 channels to be controlled individually using an Arduino microcontroller.

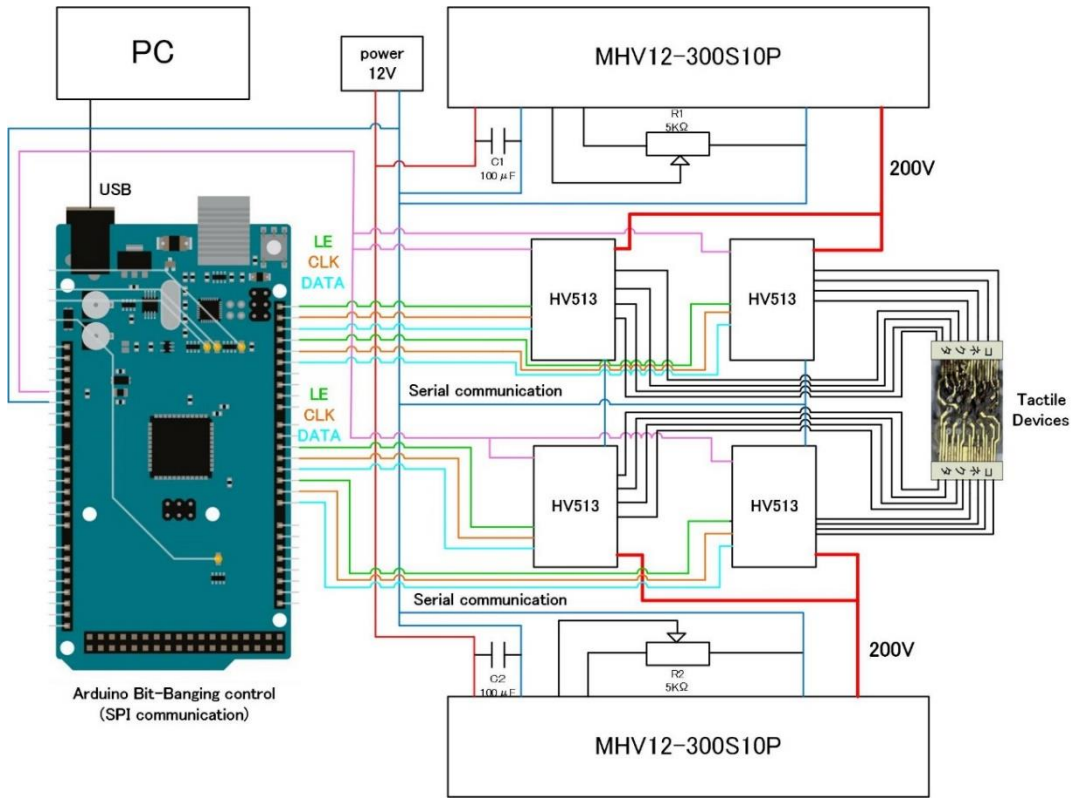


Figure 3. Overall configuration of the control system.

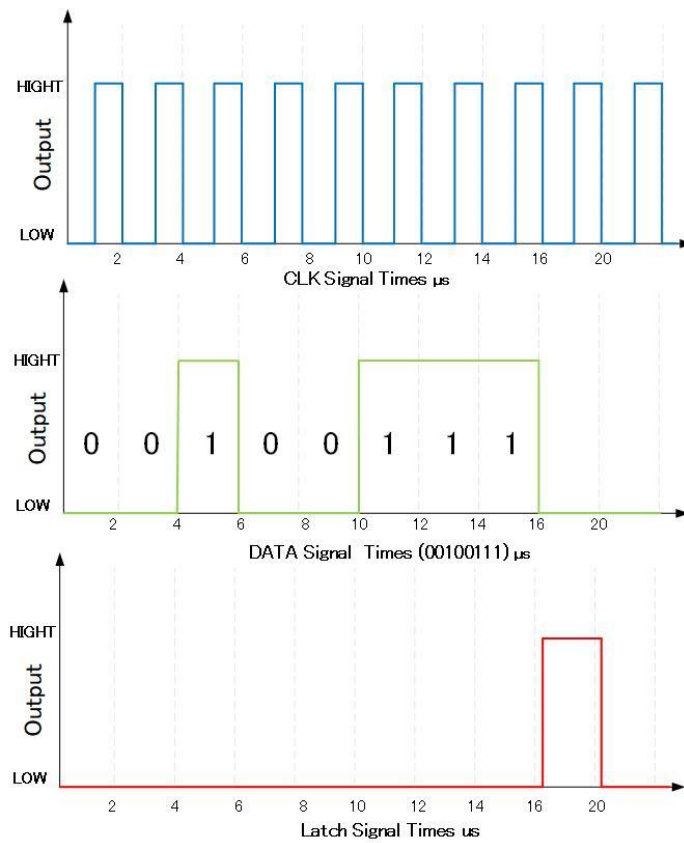


Figure 4. Signal transfer timing waveform for CLK, DATA, Latch signal.

3.2. Control panel and program of the drive circuit

A tactile generation program was developed on a PC using Visual C++ program. Figure 5 shows the button program diagram for controlling the drive circuit developed in this study. Each on/off button controls the state of eight tactile channels. Specifically, pressing the ON button sets the corresponding channel’s bit to “1” and generates vibration, while pressing the OFF button sets the bit to “0,” stopping the vibration. The message signal field displays the current 8-bit signals for the four groups, allowing users to check the signal state. The “Reset” button resets all channels, and the “All On” button turns on all channels simultaneously. Additionally, buttons within a red frame allow experimental patterns to be selected and parameters like “Time” (vibration intervals of 1 or 0.5 seconds), “Order,” and “Arrangement” to be set. Additionally, an indicator light is installed on the panel to confirm its operational status, allowing the user to verify its activity.

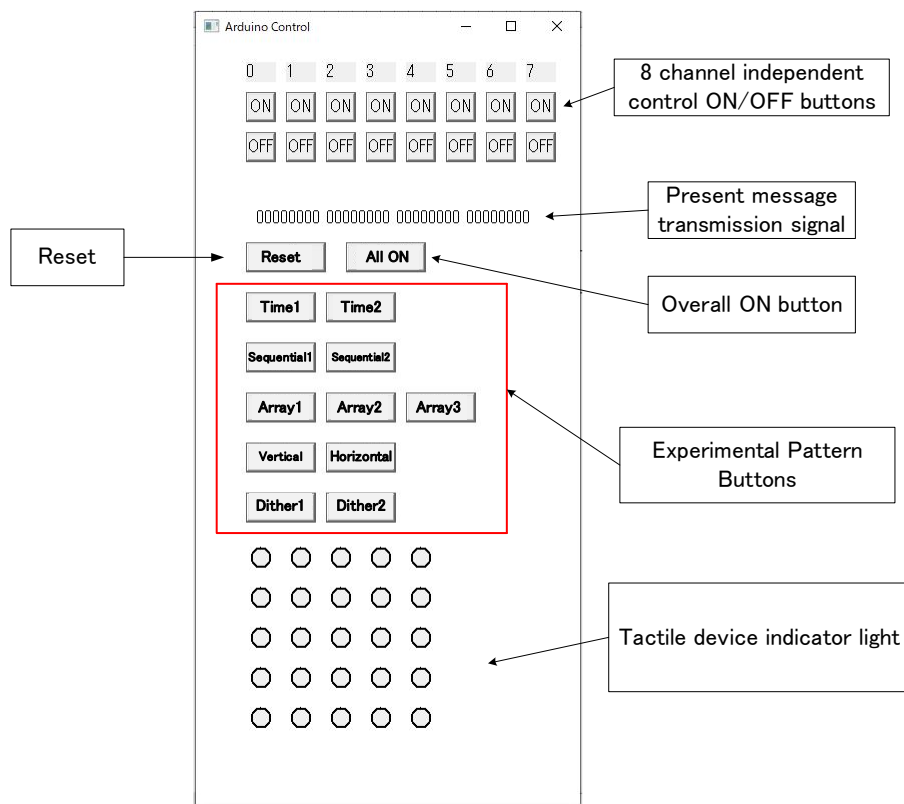


Figure 5. Button program diagram.

3.3. Tactile presentation control signal

Tactile presentation involves physical vibrations, pressure, shape and slippage to deliver tactile feedback to users. Quality depends on vibration parameters like frequency, amplitude, and duration, which, when controlled appropriately, produce diverse and complex tactile effects. In this section, we will elaborate on the basic principles of tactile presentation and the effects achieved through frequency and amplitude combinations. The key elements in tactile presentation are vibration frequency, amplitude, and duration. Adjusting these factors appropriately enables realistic tactile feedback. Frequency determines sensation sharpness or speed: low frequencies (10–100 Hz) produce slow pressing sensations, while high frequencies (100–300 Hz) yield rapid, sharp sensations [28,36,37]. Amplitude directly impacts touch intensity, with higher amplitudes indicating stronger contact and lower amplitudes suggesting gentler

touch. Duration determines the length of the tactile experience, where shorter durations feel like light touches and longer durations feel like sustained pressing. Human touch sensitivity ranges from approximately 5 Hz to 500 Hz, with peak sensitivity between 200–300 Hz. Adjusting these factors enhances realism and precision in tactile presentations in VR.

3.3.1. Stimulus of position recognition

In Arrangement 1, subjects’ ability to identify changes in stimulus positions on the tactile device is evaluated. Specifically, subjects are instructed to identify sequential changes in two columns or rows. This experiment assesses the device’s ability to clearly present static tactile patterns. Figure 6 shows three patterns used in position recognition experiments. Each pattern has different stimulus configurations, with red indicating vibration points. The Array 1 generates vibrations sequentially across 10 points on both the left and right sides. The Array 2 generates vibrations sequentially across 10 points on the top and bottom. The Array 3 vibrates in a cross pattern from a central point.

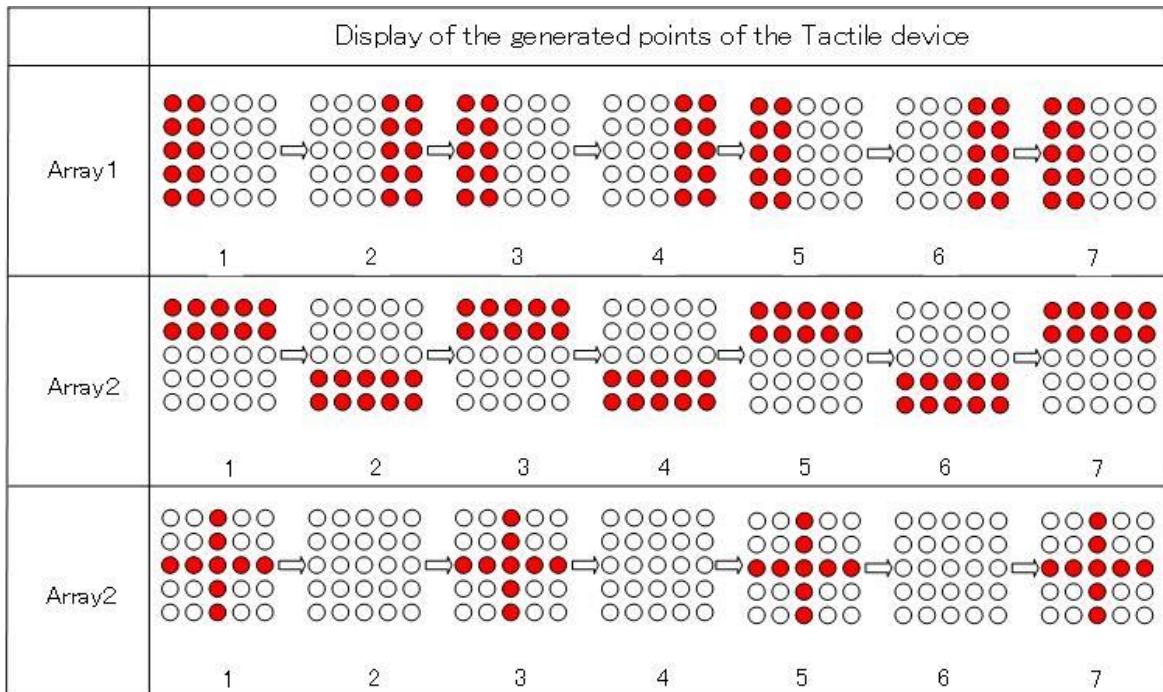


Figure 6. Three patterns of stimulus of position awareness.

Figure 7 shows the flowchart of the position change development software. When the system starts, user selects a pattern and transmits data to Arduino based on the selection. Then, the system sets the frequency to 200 Hz with a 50% duty cycle. The Arduino Mega 2560 then transmits data to HV513 via serial communication. Once HV513’s main loop begins, data processing starts, with the main loop repeating until an 8-bit data change is detected. If no data updates occur, the loop pauses, awaiting new data. When the data transfer is completed, the 8-bit data will output a voltage on the corresponding channel. The tactile device, driven by voltage and frequency settings, generates vibrations. Subjects feel the device’s vibrations.

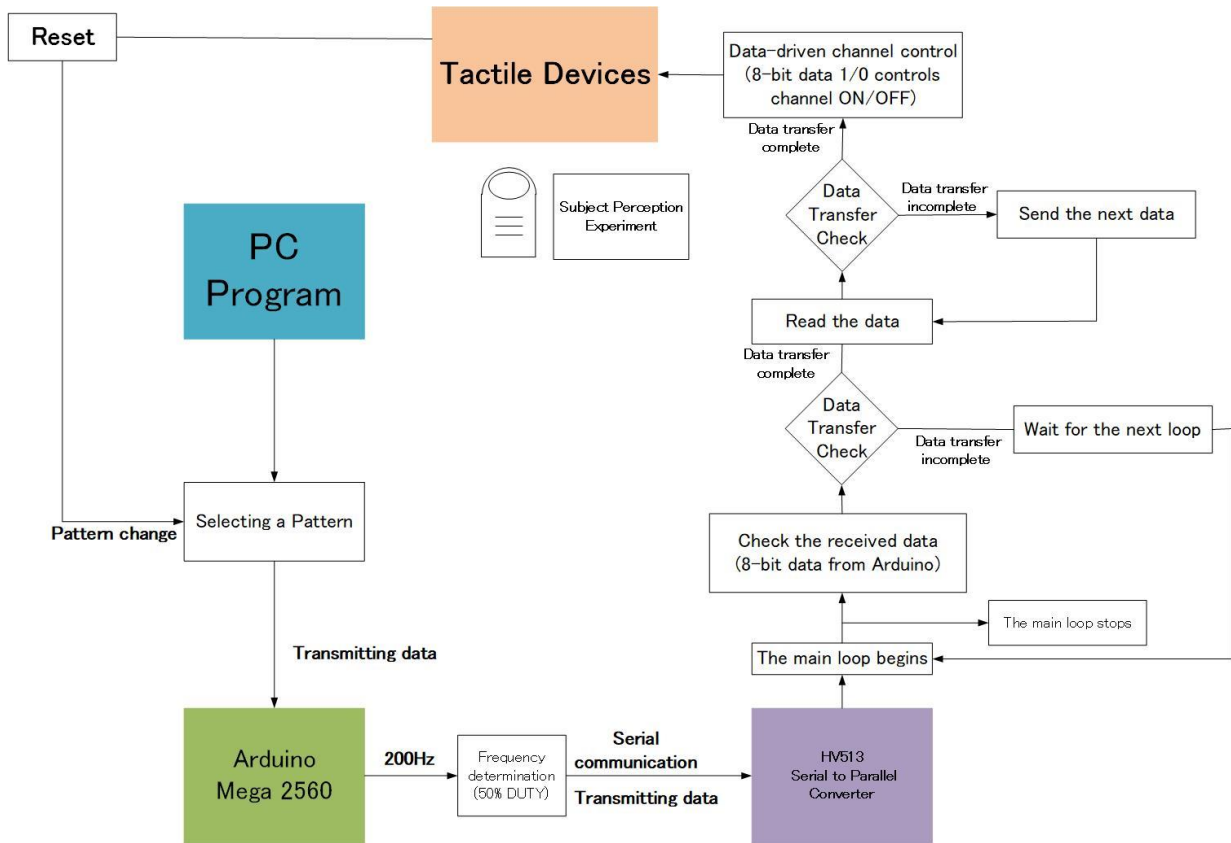


Figure 7. Flowchart of stimulus position assign.

3.3.2. Stimulus of direction change

The second stimulation method presents the direction of movement to the subject on the tactile device. This method controls the direction of movement along a column or a row. The manipulation process is shown in the flow chart of Figure 7. Figure 8 shows the pattern used to recognize the movement of stimuli. The "slide" function generates vibrations at five points simultaneously while sliding the position horizontally or downward.

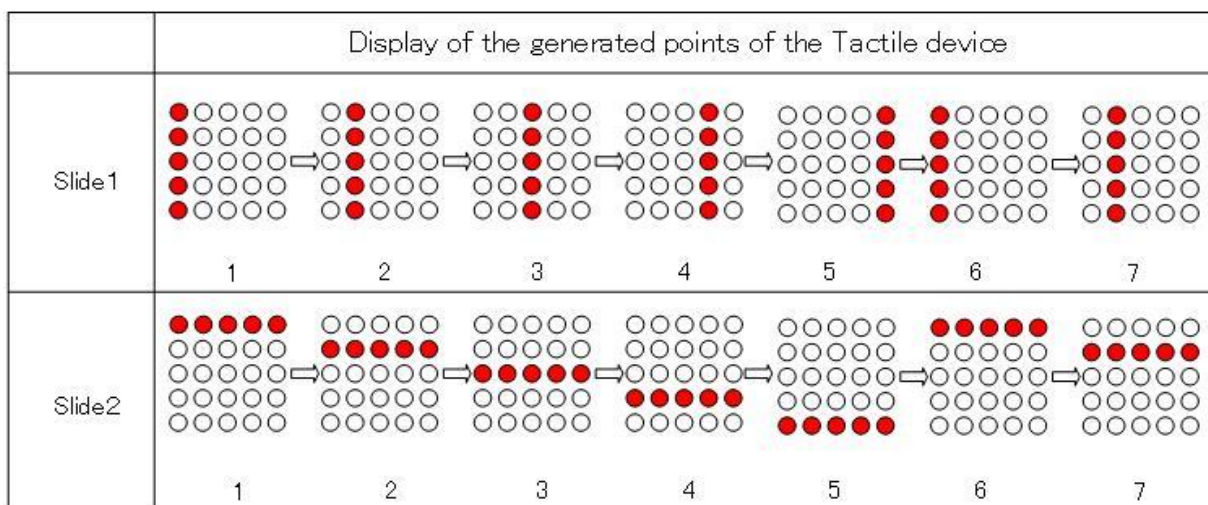


Figure 8. Patterns of stimulus of direction changing.

3.3.3. Vibration intensity and binary dithering control

Binary dithering methods produce a continuous intensity gradation. This experiment uses binary dithering to achieve different intensity levels on the tactile device. In this method, a tactile device generates multi-level haptic sensations by converting a continuous intensity gradient into vibration density, which can be controlled by adjusting the duty cycle. In this experiment, a signal is generated based on a 400 Hz square wave. Outputting a 400 Hz signal twice results in an intensity equivalent to that of a 200 Hz signal, while outputting a 400 Hz signal once results in half the vibration intensity. Figure 9 shows a 200 Hz square wave (normal intensity) and a 400 Hz dither waveform. The first two successive 400 Hz wave forms match the 200 Hz waveform, so the output is at normal intensity, but the following single 400 Hz waveforms are half intensity.

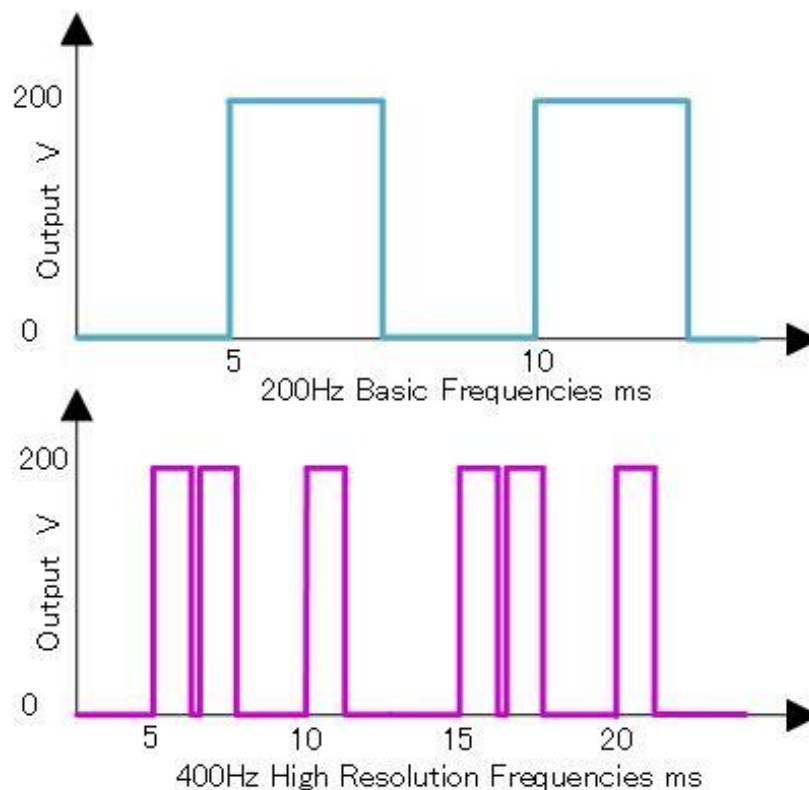


Figure 9. Waveforms used in binary dithering.

Figure 10 shows the algorithm of the binary dithering method. The dithering method selection provides two types of control with the frequency set to 400 Hz. The algorithm is the same as in Figure 7. Figure 11 shows the binary dithering based pattern with strong vibration (red) and half intensity vibration (orange). Array 1 generates a stimulus with one vertical column at half intensity, and array 2 generates a stimulus with two vertical columns at half intensity.

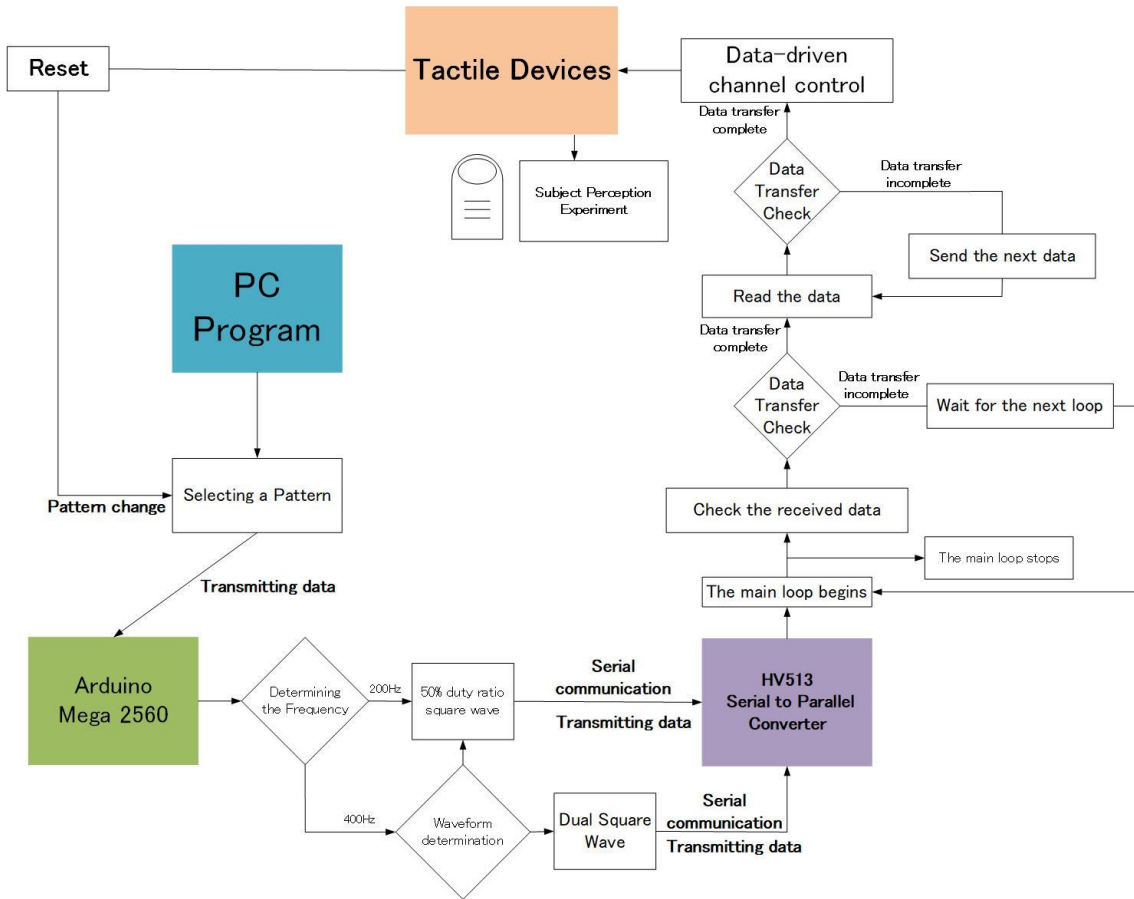


Figure 10. Flowchart for binary dithering method.

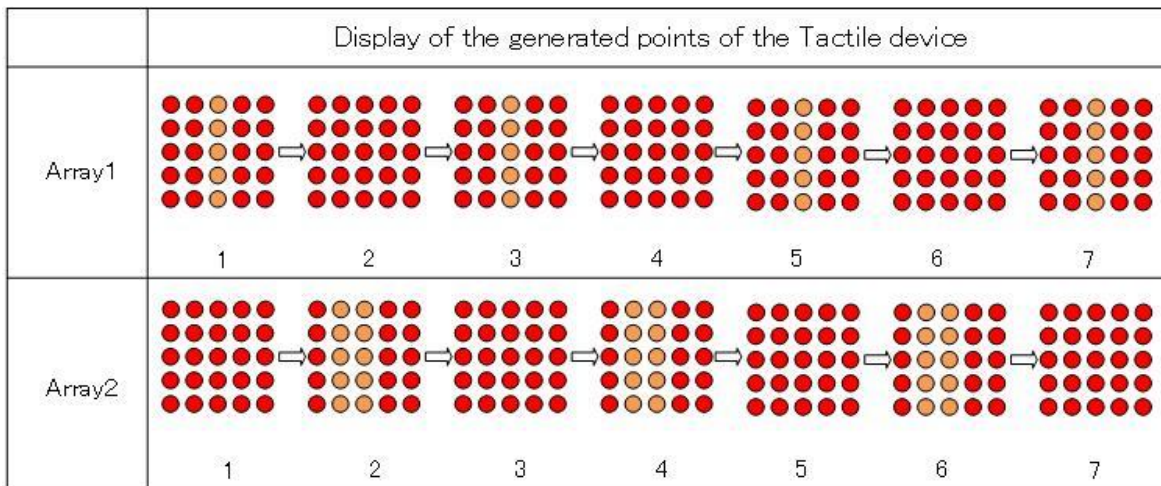


Figure 11. Patterns of binary dithering.

4. Result of generated control signal and subject experiment

With this system development, we were able to generate a signal pattern from a PC, transfer the data to the HV513 via SPI communication, and confirm the generation of a 200 V piezoelectric control signal. Here, we used 200 Hz for position recognition and 400 Hz for binary dithering-based intensity change. Figure 12 shows the waveforms of the four-channel control signals for 200 Hz position recognition, and confirmed independent control at four locations. This waveform confirmed that the tactile device could present vibrations at the correct position with accurate timing.

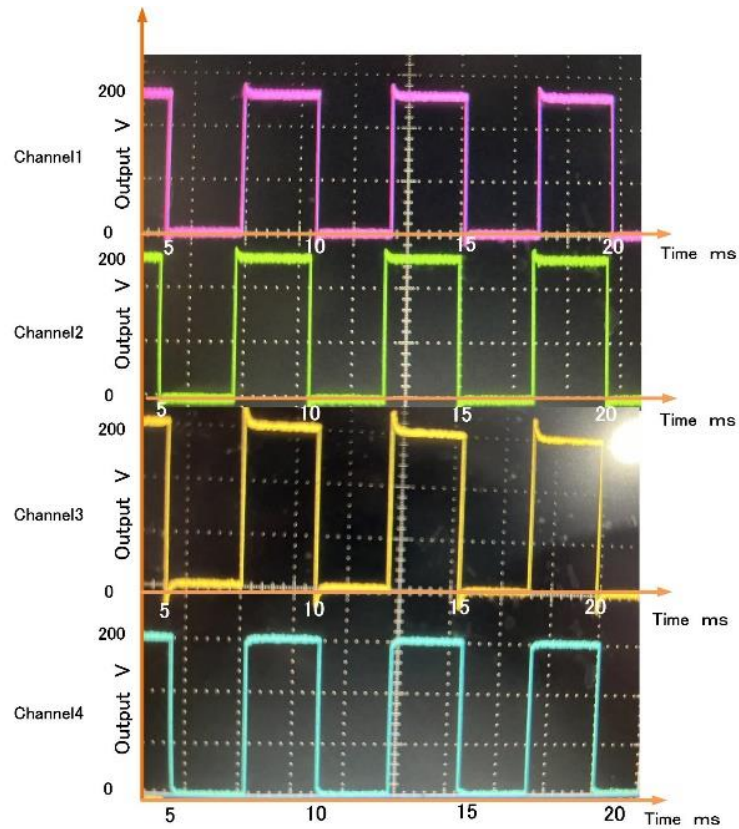


Figure 12. 4-channel position recognition waveforms at 200 Hz.

The waveform in Figure 13 shows a 400 Hz vibration presentation using the binary dithering method. The upper part (Channel 1) shows a waveform with the same intensity as 200 Hz, produced by outputting two 400 Hz waveforms simultaneously. After that, a half-intensity signal was produced by outputting 400 Hz once. This shows that intensity change is possible by dithering. The lower part (Channel 2) shows that two consecutive 400 Hz outputs are used to demonstrate the continuous output of a normal 200 Hz output. This makes it possible to reproduce multi-level vibration.

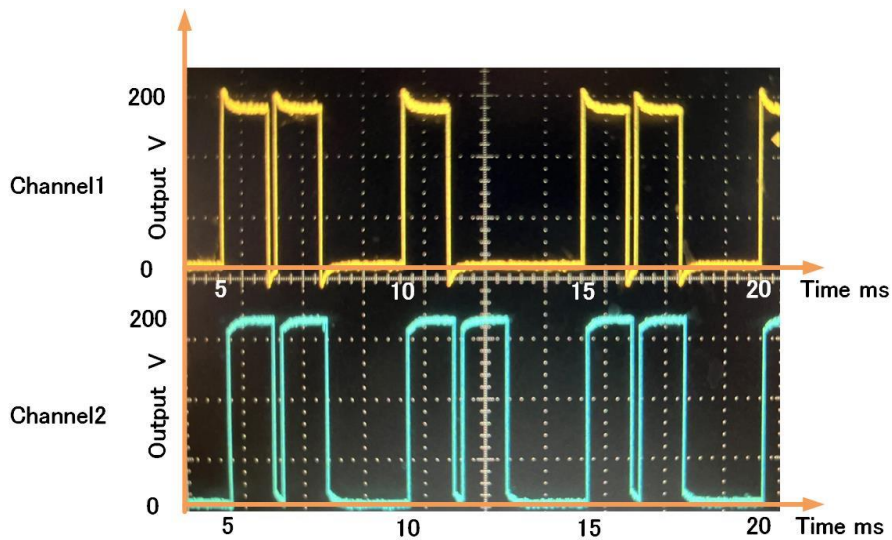


Figure 13. 400 Hz vibration intensity waveform using binary dithering method.

The experiment involved four subjects aged between 20 and 22 years old, who placed their fingers on a haptic device and conducted four types of experiments. In the first test, a normal vibration of 200 Hz was presented to two different points, and participants were asked to answer whether they could distinguish the vibration position in two cases: (1) when the two points were presented at different times, and (2) when the vibration was presented simultaneously. In the second test, a normal vibration of 400 Hz was presented at two different points, and participants were asked to answer whether they could distinguish the vibration position in two cases: (3) when the two points were presented at different times, and (4) when the vibration was presented simultaneously. Here, the 400 Hz signal shows a weak signal (dither). The finger tactile test is shown in Figure 14. The results are shown in Table 1. From these experiments, both the normal 200 Hz signal and the weak 400 Hz signal were recognized 100% of the time, and the difference in position was also recognized, verifying the effectiveness of the tactile presentation ability of this system. This result was due to the fact that the test was conducted on subjects in their 20s with high tactile sensitivity.

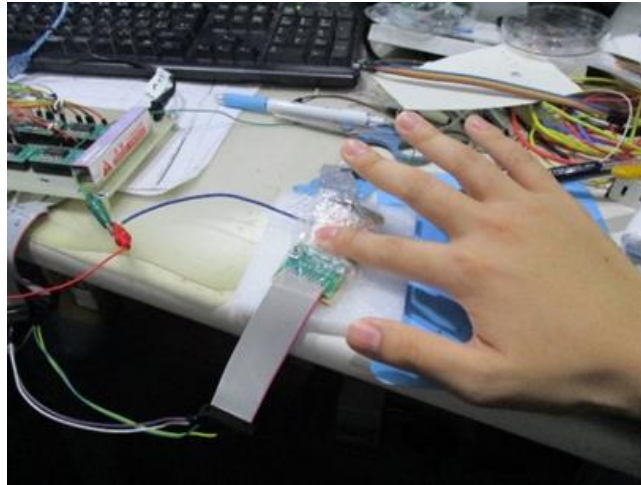


Figure 14. Finger tactile test method.

Table 1. Subject experiment on tactile sensation.

Examination content	Recognition percent [%]
(1) Vibrotactile sensations generated by a 200 Hz signal are presented at different positions with a time lag	100
(2) Vibrotactile sensations generated by a 200 Hz signal were presented simultaneously at different positions	100
(3) Vibrotactile sensations generated by a 400 Hz signal (dither: weak) are presented at different positions with a time lag	100
(4) Vibrotactile sensations generated by a 400 Hz signal (dither: weak) were presented simultaneously at different positions	100

5. Conclusion

In this study, we developed a signal generation system for a tactile presentation device that can present precise tactile sensations and movement directions based on the 200 Hz frequency, which is the

frequency at which humans have good perception. We also developed a 400 Hz-based vibration presentation method using a binary dithering method to increase the variety of tactile sensations. We conducted control experiments on the piezoelectric driver and confirmed that it was capable of responding at the required frequency and outputting multiple tones. This will enable the control of tactile devices with different frequencies and complex vibration patterns. We believe that this is the first device that a thin, multi-point tactile device with a driving power of 200 V has been developed other than for electrical stimulation. In addition, it is safe because it does not pass electric current directly through the skin.

In the future, we plan to use the tactile device to conduct subject experiments and verify the effectiveness of the tactile device and the control system. For these verifications, we plan to combine haptics and tactile technologies for applications in the metaverse, robotics, and medical applications. We believe this technology will also be important in 6G-enabled metaverse technologies [38,39,40].

Acknowledgments

We are supported by the Nanotechnology Platform and Advanced Research Infrastructure for Materials and Nanotechnology in Japan of the MEXT Japan, at the Center for Integrated Nano Technology Support, Tohoku University, and JSPS KAKENHI Grant Numbers 17K00285 and 21K12002. We thank Prof. Liwei Lin (UC Berkeley) and Toru Sai (TPU) for discussions.

Conflicts of interests

The authors declare no conflicts of interest associated with this manuscript.

Authors' contribution

Conceptualization, J. Sone; methodology, J. Sone; software, J. Zheng; validation, J. Zheng and J. Sone; formal analysis, J. Zheng and Y. Otahara; investigation, J. Zheng, Y. Otahara and J. Sone; resources, J. Sone; data curation, J. Zheng and Y. Otahara; writing—original draft preparation, J. Zheng; writing—review and editing, J. Sone; visualization, J. Zheng; supervision, J. Sone; project administration, J. Sone; funding acquisition, J. Sone. All authors have read and agreed to the published version of the manuscript.

Ethical statement

This study was approved by the ethics committee of Tokyo Polytechnic University (No.2024-11).

References

- [1] Durlach NI, Sheridan TB, Ellis SR. Human Machine Interfaces for Teleoperators and Virtual Environments. *NASA Conference Publication 10071*, Santa Barbara, United State, March 4–9, 1990, pp. 1–155.
- [2] Appino PA, Lewis JB, Koved L, Ling DT, Rabenhorst DA, *et al.* An architecture for virtual worlds. *Presence: Teleoper. Virtual Environ.* 1992, 1(1):1–17.
- [3] Costanza E, Kunz A, Fjeld M. Mixed Reality: A Survey. In *Human Machine Interaction: Research Results of the MMI Program*, Berlin, Heidelberg: Springer Berlin Heidelberg, 2009. pp. 47–68.

- [4] Tachi S, Tanie K, Komoriya K, Kaneko M. Tele-existence (I): Design and Evaluation of a Visual Display with Sensation of Presence. In *Theory and Practice of Robots and Manipulators: Proceedings of RoManSy '84: The Fifth CISM --- IFToMM Symposium*, Boston, MA: Springer US, 1985. pp. 245–254.
- [5] Maeda T, Tachi S. Space Perception Model which Generates Horopter. *Trans. Soc. Instrum. Control Eng.* 1989, 25(10): 1111–1118.
- [6] Maeda T, Arai H, Tachi S. Design and Evaluation of Binocular Head-Mounted Displays. *J. Robot. Soc. Japan* 1992, 10(5):99–109.
- [7] Oyama E, Tsunemoto N, Tachi S, Inoue Y. Experimental Study on Remote Manipulation Using Virtual Reality. *Presence* 1993, 2(2):112–124.
- [8] Tachi S, Yasuda K. Evaluation Experiments of a Telexistence Manipulation System. *Presence*. 1994, 3(1): 35–44.
- [9] Takada M, Matsuda K, Kishi N, Tachi S. A new see-through Head Mounted display with variable transparency by Electrochromic. *IEEJ Trans. Electron. Inf. Syst.* 1995, 115(2):267–272.
- [10] Hirose M, Ogi T, Ishiwata S, Yamada T. Development and evaluation of the CABIN immersive multiscreen display, *SYST COMPUT JPN.* 1999, 30(1):13–22.
- [11] Hirose M, Ogi T, Yamada T. Integrating live video for immersive environments, *IEEE Multimed.* 1999, 6(3):14–22.
- [12] Sreelakshmi M, Subash TD. Haptic Technology: A comprehensive review on its applications and future prospects, *Mater Today: Proceedings*, Part B, 2017 4(2): 4182–4187.
- [13] Chouvardas VG, Miliou AN, Hatalis MK. Tactile displays: Overview and recent advances. *Displays* 2008, 29(3):185–194.
- [14] Massie TH. Design of a Three Degree of Freedom Force-Reflecting Haptic Interface. SB Thesis, MIT, 1993.
- [15] Asano T, Yano H, Iwata H. Basic Technology of Simulation System for Laparoscopic Surgery in Virtual Environment with Force Display. *Medicine Meets Virtual Reality*, IOS Press 1997, 39:207–215.
- [16] Ishii M, Sato M. A 3D Spatial Interface Device Using Tensed Strings, *Presence* 1994, 3(1):81–86.
- [17] Hasegawa S, Sato M. Real-time Rigid Body Simulation for Haptic Interactions Based on Contact Volume of Polygonal Objects'. *Comput. Graph. Forum* 2004, 23(3):529–538.
- [18] Kim S, Hasegawa S, Koike Y, Sato M. A Proposal of 7 DOF Force Display: SPIDAR-G. *TVRSJ* 2002, 7(3):403–412.
- [19] Kohno Y, Walairacht S, Hasegawa S, Koike Y, Sato M. Evaluation to Two-Handed Multi-Finger Haptic Device SPIDAR-8. *ICAT 2001*, 135–140.
- [20] Endo T, Aoyama H, Nakagawa S, Kawasaki H. Haptic Display by a Side-Faced-Type Multi-Fingered Haptic Interface, *IFAC Proceedings* 2012, 45(22):367–372.
- [21] Sone J, Mori T, Itamoti O, Nagae T, Hasegawa S, *et al.* Development of Mechanism in Multi-finger Haptic Display-Development of haptic mechanism and fusion with Spidar. *Proceeding of ASIAGRAPH* 2008, 91–96.
- [22] Chouvardas VG, Miliou AN, Hatalis MK. Tactile displays: Overview and recent advances. *Displays* 2008, 29(3):185–194.
- [23] Purves D, Augustine GJ, Fitzpatrick D, *et al.* *Neuroscience*, 2nd ed. Sunderland (MA): Sinauer

- Associates, 2001.
- [24] Bliss JC, Katcher MH, Rogers CH, Shepard RP. Optical-to-Tactile Image Conversion for the Blind. *IEEE Trans. Man-Machine Syst.* 1970, 11(1):58–65.
- [25] Ikei Y, Wakamatsu K, Fukuda S. Vibratory tactile display of image-based textures. *IEEE Comput. Graph. Appl.* 1997, 17(6):53–61.
- [26] Hudin C. Local friction modulation using non-radiating ultrasonic vibrations. In *2017 IEEE World Haptics Conference (WHC)*, 2017, pp. 19–24.
- [27] Kajimoto H. Electrotactile Display with Real-Time Impedance Feedback Using Pulse Width Modulation. *IEEE Trans. Haptics* 2012, 5(2):184–188.
- [28] Higashi K, Okamoto S, Yamada Y, Nagano H, Konyo M. Hardness perception by tapping: Effect of dynamic stiffness of objects. In *2017 IEEE World Haptics Conference (WHC)*, 2017, pp. 37–41.
- [29] Koo IM, Jung K, Koo JC, Nam J-D, Lee YK, *et al.* Development of Soft-Actuator-Based Wearable Tactile Display. *IEEE Trans. Robot.* 2008, 24(3):549–558.
- [30] Lee HS, Phung H, Lee D-H, Kim UK, Nguyen CT, *et al.* Design analysis and fabrication of arrayed tactile display based on dielectric elastomer actuator. *Sensors Actuators A Phys.* 2014, 205:191–198.
- [31] Sone J, Sato T, Yanagawa S, Yamada K, Lin L. Study of Thin Polymer pre-charge Multi point Tactile device. In *2022 IEEE Conference on Virtual Reality and 3D User Interfaces Abstracts and Workshops (VRW)*, 2022, pp. 316–318.
- [32] Sone J. Fingertip tactile sensation via piezoelectric micromachined ultrasonic transducers with an amplified interface. *Sci. Rep.* 2024, 14(1):2629.
- [33] Harris SL, Harris DM. *Digital Design and Computer Architecture*; Harris SL, Harris DM, Eds. Burlington: Morgan Kaufmann, 2022.
- [34] Ikei, Y., *et al.* Multilevel sensation intensity presentation methods on tactile displays. *Trans. Jpn. Soc. Mech. Eng. C*, 2000, 66(644): 194–200.
- [35] Zhong J, Ma Y, Song Y, Zhong Q, Chu Y, *et al.* A Flexible Piezoelectret Actuator/Sensor Patch for Mechanical Human–Machine Interfaces. *ACS Nano* 2019, 13(6):7107–7116.
- [36] Kajimoto H, Jones LA. Wearable Tactile Display Based on Thermal Expansion of Nichrome Wire. *IEEE Trans. Haptics* 2019, 12(3):257–268.
- [37] Ikei, Y., Watanabe, H., & Fukuda, K. Vibratory touch display for tactile feeling of surface roughness. *Proceedings of IEEE Virtual Reality Annual International Symposium (VRAIS)*, 1997: 293-300.
- [38] Adil M, Song H, Khan MK, Farouk A, Jin Z. 5G/6G-enabled metaverse technologies: Taxonomy, applications, and open security challenges with future research directions. *J. Netw. Comput. Appl.* 2024, 223:103828.
- [39] Chowdary A, Bazzi A, Chafii M. On Hybrid Radar Fusion for Integrated Sensing and Communication. *IEEE Trans. Wirel. Commun.* 2024, 23(8):8984–9000.
- [40] Wang D, Bazzi A, Chafii M. RIS-Enabled Integrated Sensing and Communication for 6G Systems. In *2024 IEEE Wireless Communications and Networking Conference (WCNC)*, 2024, pp. 1–6.